



Fermi National Accelerator Laboratory

FERMILAB-Pub-91/299-E

E760

Precision Measurements of Charmonium States formed in $\bar{p}p$ Annihilation

The E760 Collaboration

*Fermi National Accelerator Laboratory
P.O. Box 500, Batavia, Illinois 60510*

November 1991

* Submitted to *Physical Review Letters*.



Operated by Universities Research Association Inc. under Contract No. DE-AC02-76CHO3000 with the United States Department of Energy

Precision Measurements of Charmonium States formed in $\bar{p}p$ Annihilation

T.A. Armstrong⁶, D. Bettoni², V. Bharadwaj¹, C. Biino⁷, G. Borreani²,
D. Broemmelsiek⁴, A. Buzzo³, R. Calabrese², A. Ceccucci⁷, R. Cester⁷,
M.D. Church¹, P. Dalpiaz², P.F. Dalpiaz², J.E. Fast⁴, S. Ferroni³,
C.M. Ginsburg⁵, K.E. Gollwitzer⁴, A.A. Hahn¹, M.A. Hasan⁶, S.Y. Hsueh¹,
R.A. Lewis⁶, E. Luppi², M. Macri³, A. Majewska⁶, M.A. Mandelkern⁴,
F. Marchetto⁷, M. Marinelli³, J.L. Marques⁴, W. Marsh¹, M. Martini²,
M. Masuzawa⁵, E. Menichetti⁷, A. Migliori⁷, R. Mussa⁷, S. Palestini⁷,
N. Pastrone⁷, C. Patrignani³, J. Peoples, Jr.¹, L. Pesando⁷, F. Petrucci²,
M.G. Pia³, S. Pordes¹, P.A. Rapidis¹, R.E. Ray^{5,1}, J.D. Reid⁶, G. Rinaudo⁷,
J.L. Rosen⁵, A. Santroni³, M. Sarmiento⁵, M. Savrié², J. Schultz⁴,
K.K. Seth⁵, G.A. Smith⁶, L. Tecchio⁷, F. Tommasini³, S. Trokenheim⁵,
M.F. Weber⁴, S.J. Werkema¹, J.L. Zhao⁵, M. Zito³.

¹*Fermi National Accelerator Laboratory, Batavia, Illinois 60510, USA*

²*I.N.F.N. and University of Ferrara, 44100 Ferrara, Italy*

³*I.N.F.N. and University of Genoa, 16146 Genoa, Italy*

⁴*University of California at Irvine, California 92717, USA*

⁵*Northwestern University, Evanston, Illinois 60201, USA*

⁶*Pennsylvania State University, University Park, Pennsylvania 16802, USA*

⁷*I.N.F.N. and University of Turin, 10125 Turin, Italy.*

P.A.C.S. numbers 13.75 Cs, 14.40Jz

Disclaimer

This report was prepared as an account of work sponsored by an agency of the United States Government. Neither the United States Government nor any agency thereof, nor any of their employees, makes any warranty, express or implied, or assumes any legal liability or responsibility for the accuracy, completeness, or usefulness of any information, apparatus, product, or process disclosed, or represents that its use would not infringe privately owned rights. Reference herein to any specific commercial product, process, or service by trade name, trademark, manufacturer, or otherwise, does not necessarily constitute or imply its endorsement, recommendation, or favoring by the United States Government or any agency thereof. The views and opinions of authors expressed herein do not necessarily state or reflect those of the United States Government or any agency thereof.

Abstract

Fermilab experiment E-760 studies the resonant formation of Charmonium states in proton-antiproton interactions using a hydrogen gas-jet target in the antiproton Accumulator ring at Fermilab. Precision measurements of the mass and width of the Charmonium states, χ_1 , χ_2 , the first direct measurement of the ψ' width and a new precision measurement of the J/ψ mass are presented.

We report the first results from Fermilab experiment E-760, a study of charmonium states formed directly in proton-antiproton annihilation. We present the first measurement of the total width of the χ_1 (3P_1), and improved measurements of the χ_2 (3P_2) total width, and of the masses of both resonances. We also report the first direct measurement of the total width of the ψ' and a new measurement of the mass of the J/ψ .

The experiment uses a beam of antiprotons circulating in the Fermilab Antiproton Accumulator ⁽¹⁾ and an internal hydrogen gas-jet target to study charmonium states formed in the exclusive reaction $\bar{p} + p \rightarrow (\bar{c}c)$, a technique first exploited at the CERN ISR ⁽²⁾. States of all allowed J^{PC} are formed directly in $\bar{p}p$ annihilation while only states of $J^{PC} = 1^{--}$ are made directly in e^+e^- annihilation. In $\bar{p}p$ annihilations, however, the $(\bar{c}c)$ formation cross sections are as small as one part in 10^6 of the total cross section and it is not feasible to detect these states through their hadronic decays. Nevertheless, by selecting the decay modes: $\bar{c}c \rightarrow J/\psi + X$, $J/\psi \rightarrow e^+e^-$ an almost background free sample can be obtained.

The masses and widths of the $(\bar{c}c)$ states are determined directly from the antiproton beam energy by measuring the excitation curves of the resonances as the energy of the antiproton beam is changed in small steps. The resonances were scanned by decelerating the antiproton beam from the accumulation energy of 8.9 GeV to an energy just above the resonance and then decelerating in steps of between 170 and 500 keV (center of mass energy) depending on the resonance. In the present experiment, the antiproton beam

was cooled to $(\Delta p/p)_{rms} \approx 2 \times 10^{-4}$. This produced a spread in the center of mass energy, ΔW , of 240 keV thus allowing the first direct measurement of sub-MeV widths for the charmonium states.

The results presented here depend on our knowledge of two parameters of the antiproton beam: the absolute value of the beam momentum and the beam momentum spread. The beam momentum is most precisely derived from the beam velocity measured from the revolution frequency, f_r and the orbit length, L_o . Since the revolution frequency is measured with a precision of approximately 2 parts in 10^7 , the major uncertainty in determining the velocity of the beam comes from the knowledge of the orbit length. Conventional surveying techniques proved not sufficiently precise and so a reference orbit length, L_{ref} was determined by performing an energy scan at the ψ' and taking the value of the ψ' mass from the literature. The 0.1 MeV/c² uncertainty in this mass⁽³⁾ produces a 0.7 mm systematic uncertainty in L_{ref} .

Repeated scans at the J/ψ showed a reproducibility of the center of mass energy setting to better than 0.05 MeV/c² which corresponds to a further uncertainty of 1 mm in the total orbit length of 474.046 meters. This is consistent with the intrinsic resolution of the beam position monitors which are used to correct for small changes between the reference orbit and the orbits actually used in the scans of the resonances.

To determine the true resonance widths, the beam momentum distribution must be unfolded from the observed excitation curves. This distribution is derived from the beam revolution frequency spectrum using the relation $\Delta p/p = (1/\eta) \times \Delta f_r/f_r$ where η depends on the setting of the Accumulator lattice. The beam revolution frequency spectrum itself is obtained with high precision by Fourier analysis of the beam current Schottky noise.

For the χ_1 and the χ_2 , the resonance width is significantly larger than ΔW and the value of η is obtained with sufficient precision from the measured synchrotron oscillation frequency. Our experiment also yields a direct measurement of the ψ' width even though the energy spread of the beam is larger than the width of the resonance. This result is due to the properties

of the convolution of a Breit-Wigner with a Gaussian distribution. As an example, the observed peak cross section for $\Gamma_{Beam} > \Gamma_{Res.}$ is approximately

$$\sigma_{peak} \approx \sqrt{4\ln 2/\pi} \times A/\Gamma_{Beam} \times (1 - \sqrt{4\ln 2/\pi} \Gamma_{Res.}/\Gamma_{Beam})$$

where A is the integral of the resonance cross section. The bracketed term shows that the resonance width has a linear effect on the observed peak cross section. For $\Gamma_{Res.}/\Gamma_{Beam} \ll 1$, this term is 1 and the observed peak cross section depends only on the beam energy spread. In our case, however, this term is 0.6 at the ψ' and a direct measurement of $\Gamma_{\psi'}$ can be obtained from the shape of the excitation curve. Here a precise knowledge of η is essential, and a novel “double-scan” technique⁽⁴⁾ was developed to give a second and independent measurement of its value. In this technique, the deceleration for each energy step through the scan was performed in two stages. The first stage involved measuring the resonance cross section with the beam at a known energy, E_c^i , on the central orbit of the Accumulator. The beam was then decelerated one step without changing the Accumulator magnetic field. The deceleration reduced the beam energy by an amount ΔE , changed the revolution frequency by an amount Δf_r^i and moved the beam onto a “side” orbit where the cross section at this new energy, E_s^i , was again measured. The Accumulator magnetic field was then reduced to return the beam to the central orbit, the cross section measured and the process repeated throughout the resonance scan. The data obtained thus consists of a set of cross section measurements at known energies, E_c^i , and a second set measured at energies E_s^i where $E_s^i = E_c^i + (1/\eta)\gamma m_p \beta^2 \Delta f_r^i/f_r^i$. The value of η is found, in essence, by forcing the excitation curve from the side-orbit data to match the central orbit curve. The value of η thus obtained agrees well with the value from the synchrotron frequency measurement.

Figure 1 shows a cut through the E-760 apparatus⁽⁵⁾. The intersection of the gas-jet and the antiproton beam produces an interaction region about 0.5 cm on a side. The detector has a large acceptance and is optimized for the identification of electromagnetic final states from charmonium decay. It

covers the complete azimuth, (ϕ), and from 2° to 70° in polar angle (θ). The central and forward calorimeters identify electrons and photons and measure their energies and directions. The central calorimeter covers the region $12^\circ < \theta < 70^\circ$. The apparatus inside it consists from the beam-pipe out of: an inner scintillation-counter hodoscope, two layers of longitudinal straw-tubes which provide information in both ϕ and θ , a radial projection chamber (RPC) and an MWPC with cathode readout to provide θ information, a second scintillation-counter hodoscope and a multi-cell threshold Cerenkov counter for electron identification. The outermost tracking devices in the central region are two layers of Larocci tubes with cathode read-out for θ and ϕ information ($68^\circ > \theta > 22^\circ$), and a planar MWPC ($18^\circ > \theta > 10^\circ$). The central electromagnetic calorimeter itself consists of a cylindrical array of 1280 lead-glass Cerenkov counters each pointing to the interaction region. The forward region ($2^\circ < \theta < 12^\circ$) is instrumented with an 8 element hodoscope, and a 144 channel Pb/Scintillator calorimeter preceded by three planes of straw-tubes. An array of silicon detectors covering the polar angle region from 82° to 90° measures the yield of elastic recoil protons and provides the luminosity monitor.

The experiment trigger for this data was designed to select all ($c\bar{c}$) decays to a final state with a J/ψ decaying to e^+e^- in the acceptance of the central calorimeter. This was implemented by requiring two electron “tracks” as defined by the hodoscopes and the appropriate cells in the Cerenkov counters and two high energy clusters in the central electromagnetic calorimeter.

The invariant mass of the candidate electron-positron pair, m_{ee} , was calculated from measured cluster energies and track angles. The event selection was based on the final state topology and electron quality ‘definition’ depending on the resonance. For events found at the J/ψ formation energy the simple requirement of exactly two clusters in the central calorimeter was sufficient to obtain a clean J/ψ sample as is evident from the reconstructed mass distribution of Figure 2(a). For the χ states remarkably clean signals are found in the channel $\chi \rightarrow J/\psi + \gamma$, $J/\psi \rightarrow e^+e^-$ by performing a kine-

matic fit to the 3-body final state. Figure 2(b) shows the m_{ee} distribution for events which satisfy the kinematic fit in the χ_2 energy scan. Finally, the ψ' sample relied only on the identification of two good electron candidates obtained by cuts on the amplitudes of the signals from the hodoscopes, the RPC and the Cerenkov counters and on the shape of the calorimeter energy deposition. Figure 2(c) shows the m_{ee} distribution for events found at the ψ' formation energy. The two peaks correspond to the inclusive decay $\psi' \rightarrow J/\psi + X$, $J/\psi \rightarrow e^+e^-$ and the exclusive decay $\psi' \rightarrow e^+e^-$. The background event distribution obtained from data taken off-resonance, normalized to the on-resonance luminosity, is just visible as the solid area on Fig. 2(c). Table I lists the luminosity taken at each resonance, the total number of events found and the estimated number of background events under the resonance.

The masses and widths of the χ_1 and χ_2 states are calculated by a maximum likelihood fit of the number of events found at each point of the energy scan to the Breit-Wigner cross section convoluted with the measured beam energy distribution plus a constant background. For the ψ' , the fit uses the data from both the central and the side orbits simultaneously to yield η directly as well as the resonance width. Figure 3 shows the excitation cross sections measured with energy scans at the χ_1 , χ_2 and ψ' . The solid lines are the convolution of the resonance Breit-Wigner with the beam energy distribution; the dashed lines show a typical center of mass energy spectrum.

The results of the fits are given in Table II. For the mass measurements, the first error given is statistical, the second is the systematic error which arises from the uncertainty in the mass of the ψ' and the 1 mm resolution in the measurement of the orbit length. Since the two χ masses are so close, the mass difference, $M_{\chi_2} - M_{\chi_1}$, is hardly affected by the uncertainty in the ψ' mass. For the width measurements, the first error given is again statistical and the second systematic. For the χ states, the systematic error is due to the uncertainty in determining η and thus the beam momentum spread. For the ψ' , the effect of the uncertainty in η is included in the statistical

error of the fit to the double-scan data; the systematic uncertainty arises from the treatment of the beam frequency spectrum and from variations in the central orbit length. The effects of radiation in the initial state on the observed masses and widths are much smaller than the errors quoted and no corrections have been applied.

The uncertainty in the reference orbit length contributes only $33 \text{ keV}/c^2$ to the systematic error in the mass of the J/ψ and results in a measurement with slightly better accuracy than previously reported⁽³⁾. For the masses of the χ_2 and χ_1 the new values agree well with previous ones and the errors are reduced by a factor more than two. The width of the χ_1 has been measured for the first time and the uncertainty on the χ_2 width has been reduced from $\sim 40\%$ to $\sim 10\%$. The measurements of these total widths can be used to obtain the partial widths for radiative and hadronic decays. A comparison of these partial widths with theoretical predictions will be presented elsewhere⁽⁵⁾. Our value for the ψ' width, derived from the shape analysis of the excitation curve, is somewhat higher than the value obtained at e^+e^- machines which is derived from integrated cross-section measurements.

We gratefully acknowledge the technical support from our collaborating institutions and the outstanding contribution of the Fermilab Accelerator Division Antiproton department. This work was funded by the U.S. Department of Energy, the National Science Foundation and by the Italian Istituto Nazionale di Fisica Nucleare.

References

1. J. Peoples Jr., in Low Energy Antimatter, Workshop on the Design of a Low Energy Antimatter Facility, October 1985, ed. D. Cline, p. 144, World Scientific Publishing Co., 1986.
2. C. Baglin *et al.*, Nucl. Phys. **B286**, 592 (1987).

3. A.A. Zholentz *et al.*, Phys. Lett. **96B**, 214 (1980).
4. M. Church *et al.*, FERMILAB TM-1760, to appear in the Proceedings of the 1991 I.E.E.E. Particle Accelerator Conference, May 6-9, San Francisco.
5. T.A. Armstrong *et al.*, "Study of the χ_1 and χ_2 Charmonium States Formed in $\bar{p}p$ Annihilations" , FERMILAB-Pub-91/213-E, submitted to Nucl. Phys. B.
6. Review of Particle Properties, Phys. Lett.**B239** (1990)

Table I: Data for each resonance scan

Resonance	P_{beam} (MeV/c)	Luminosity (nb) ⁻¹	Total No. of Events	Estimated Background
J/ψ	4066.	360	~ 4000	8 ± 3
χ_1	5550.	1030	503	19 ± 3
χ_2	5724.	1160	569	22 ± 4
ψ'	6232.	990	1197	18 ± 4

Table II: Resonance parameters

Resonance	Mass (MeV/c ²)	Width (keV)
J/ψ (this expt.)	3096.88 ± 0.01 ± 0.06	
J/ψ (ref. 6)	3096.93 ± 0.09	68 ± 10
χ_1 (this expt.)	3510.53 ± 0.04 ± 0.12	880 ± 110 ± 80
χ_1 (ref. 6)	3510.6 ± 0.5	< 1300
χ_2 (this expt.)	3556.15 ± 0.07 ± 0.12	1980 ± 170 ± 70
χ_2 (ref. 6)	3556.3 ± 0.4	2600 ⁺¹²⁰⁰ ₋₉₀₀
ψ' (this expt.)	3686.0 (input)	312 ± 36 ± 12
ψ' (ref. 6)	3686.0 ± 0.1	243 ± 43
$\chi_2 - \chi_1$ (this expt.)	45.62 ± 0.08 ± 0.12	

Figure Captions

- (a) FIG. 1. A cut through the E-760 Detector
- (b) FIG. 2. The reconstructed invariant mass of candidate electron pairs for events at: (a) the J/ψ formation energy, (b) the χ_2 formation energy and (c) the ψ' formation energy (open area) and just off-resonance normalized to the same luminosity (solid area)
- (c) FIG. 3. The measured cross section for the energy scan at: (a) the χ_1 , (b) the χ_2 , (c) the ψ' . The solid line represents the best fit to the data. The dashed line shows a typical center of mass energy distribution (arbitrary vertical units)

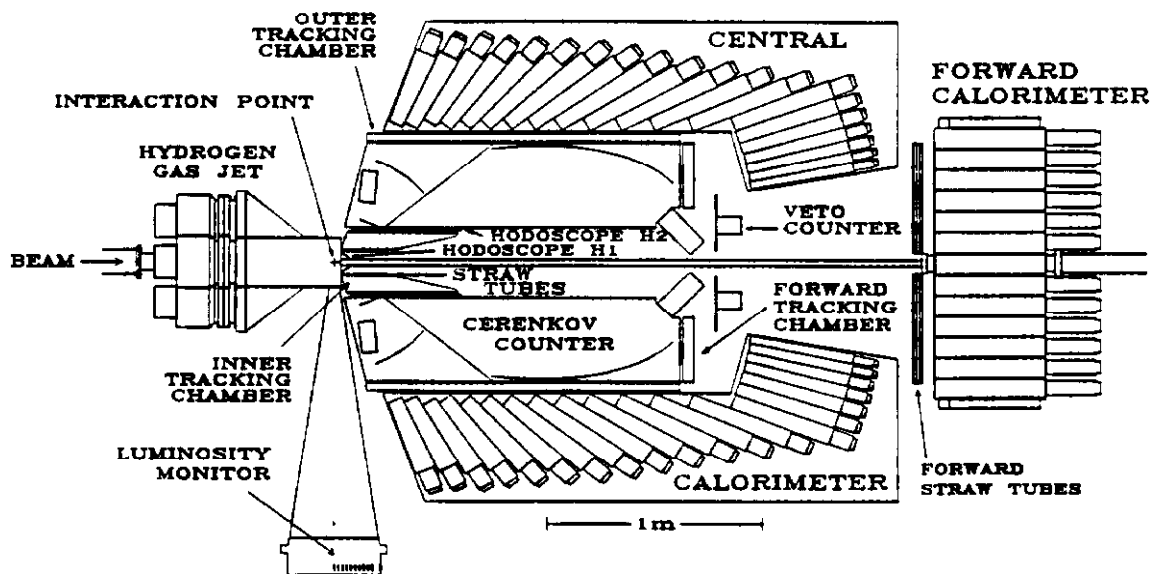


FIG 1. A cut through the E-760 Detector

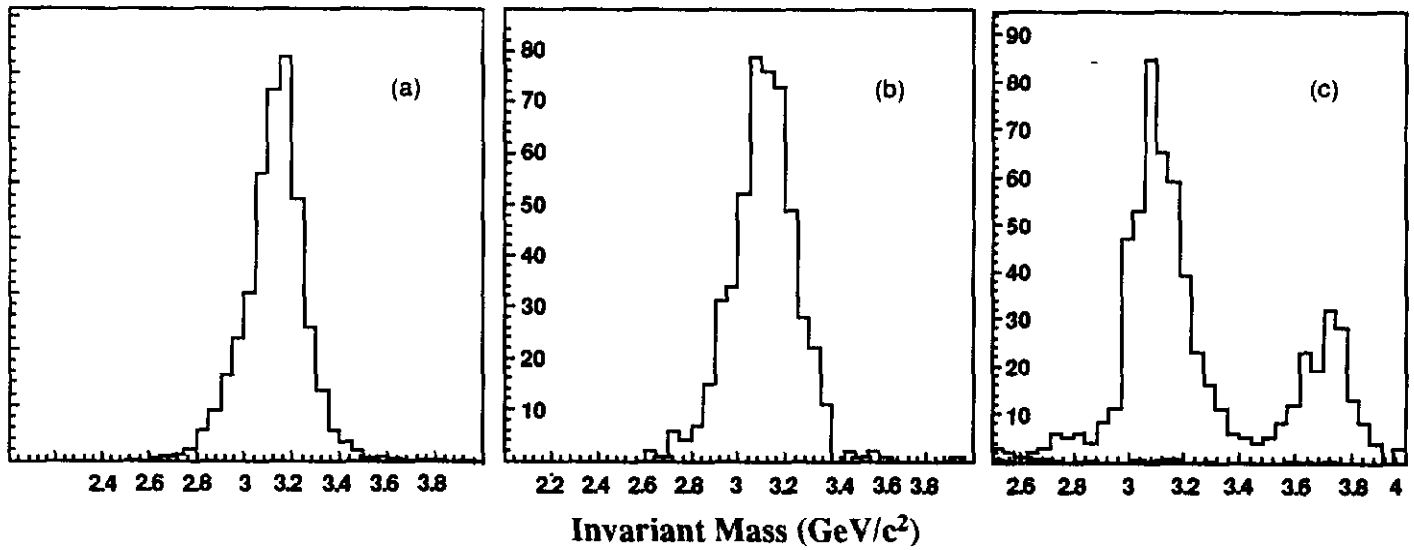


FIG. 2. The reconstructed invariant mass of candidate electron pairs for events at: (a) the J/ψ formation energy, (b) the χ_2 formation energy, and (c) the ψ' formation energy (open area) and just off-resonance normalized to the same luminosity (solid area).

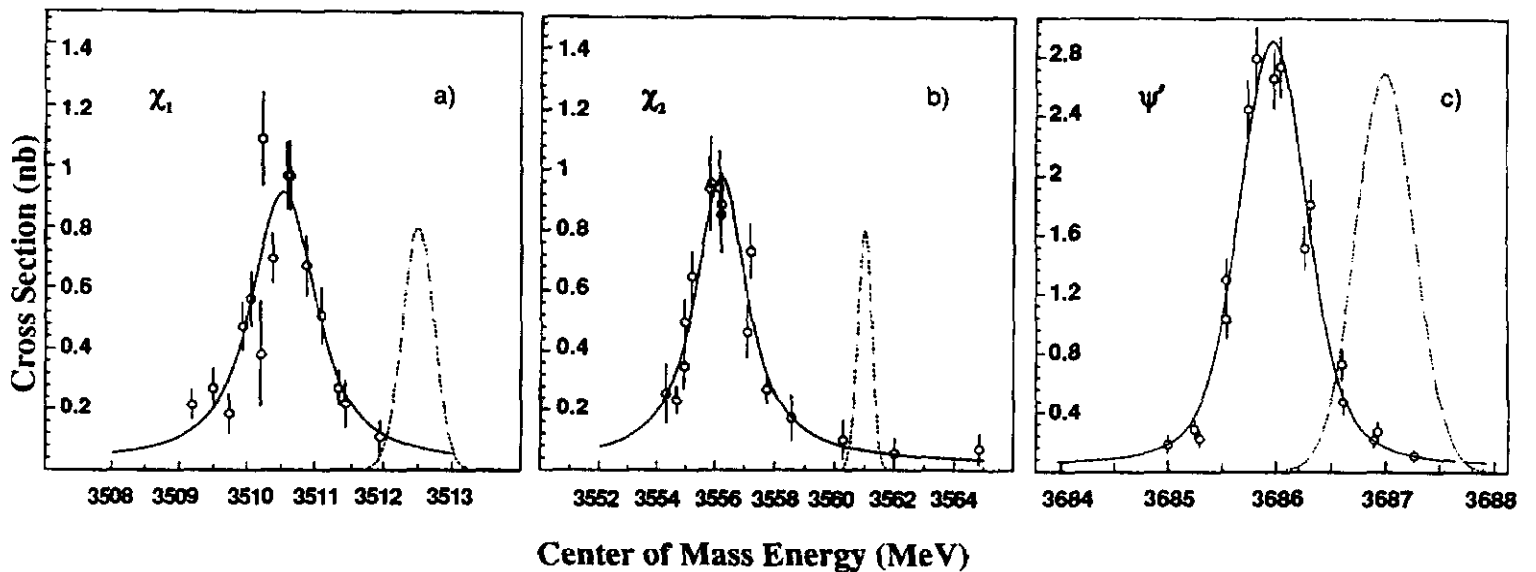


FIG. 3: Measured cross section for the energy scan at the a) χ_1 , b) χ_2 , c) ψ' . The solid line represents the best fit to the data. The dashed curve shows a typical center of mass energy distribution (arbitrary vertical units).